

# The Study of Asynchronous Motors Behavior in Artificial Load

Ion Vlad\*, Aurel Campeanu\*, Sorin Enache\*, Mihaela Tita\*

\*University of Craiova/Faculty of Electrical Engineering, Craiova, Romania, ivlad@em.ucv.ro

\*University of Craiova/Faculty of Electrical Engineering, Craiova, Romania, acampeanu@em.ucv.ro

\*University of Craiova/Faculty of Electrical Engineering, Craiova, Romania, senache@em.ucv.ro

\*University of Craiova/Faculty of Electrical Engineering, Craiova, Romania, mtita@em.ucv.ro

**Abstract** - The performances and heating of asynchronous motor are established to nominal load into a testing laboratory. Only in this way can be created real life working conditions, but there are also two big disadvantages: the need of applying a mechanical load to the shaft and the big energy consumption. Heating testing using this method is expensive and long lasting. That is why Ytterberg proposes a new method of heating test, the method of two frequencies, a synthetic form of charging. In this case, the asynchronous motor that is tested is not mechanically coupled, is powered from a network composed by a two different source of voltage and frequency which are electrically in series. Starting from machine parameters, through numerical calculations, in the paper is established the correlation of frequency and voltage of the two sources to obtain current and the same losses as the nominal regime when the motors operates without load. The speed of asynchronous machine oscillates around the synchronism speed, the power is changing very often the sign because and as result also the functioning regime as motor or alternator. Through this periodical change it creates the artificial load. Particular simulation cases are showing the internal behavior, electrical and magnetic loads to which the machine is submitted. All this reasons justified very well by simulations, are showing that we are in presence of an important distortion regime.

**Keywords** - asynchronous motors, test, numerical simulation

## I. INTRODUCTION

The performance of asynchronous machine can be obtained by applying the direct method, when the machine is loaded through the shaft at nominal torque, same as in real function conditions. During this test there are performed several determinations, including heating test of the machine. It is very important that the heating test is done on a test bench. As a result is becoming more advantageous to use a simpler method of heating testing the two frequency method designed by A. Ytterberg [7], [9].

Using this method at testing asynchronous machines has the following advantages against the known standard methods: it is applicable for all range of machines, including the vertical ones, it is applicable for all range of powers, doesn't require shaft coupling with another machine.

## II. DEFORMING REGIME FOR THE METHOD OF TWO FREQUENCIES

The asynchronous motor which is tested MAS is not mechanically coupled, which represents a big advantage. The machine is powered from two sources with different

outputs and frequency- synchronous alternators  $GS_I$  and  $GS_{II}$ , connected in series (fig.1).

Through the change of the speed and excitation currents of the two sources is ensured the frequencies  $f_I$ ,  $f_{II}$  and the voltages  $U_I$ ,  $U_{II}$  for the right values used for the tests.

The voltage has a periodic variation with frequency  $f$  which allows decomposition in harmonic series and analysis of the phenomena. From the point of view of the deforming regime [2-5], [7], [16] the essential problem is to analyze the current and voltage waveforms associated to the motor power, highlighting major harmonics and harmonic analysis of factors known.

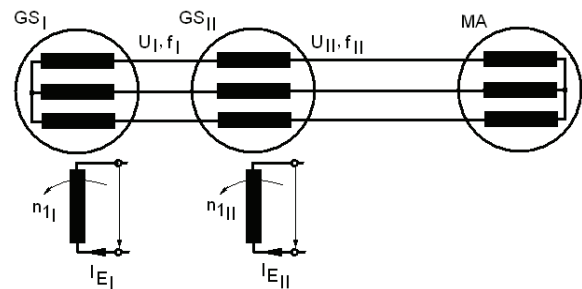


Fig. 1. Schematic diagram of the method of two frequencies.

For this study is considered the asynchronous motor equations, written in complex and the T equivalent circuit, from which is resulting the impedance and current as a measure of the answer. In the case of the asynchronous machine which is tested (fig. 1), the feeding voltage is harmonic:

$$u = \sqrt{2} U_1 \sin(\omega_1 t + \alpha_1) + \sqrt{2} U_2 \sin(\omega_2 t + \alpha_2) \quad (1)$$

Using numerical methods of decomposition voltage harmonic form is obtained:

$$u = \sum_{k=1}^{\infty} \sqrt{2} U_k \sin(k\omega t + \alpha_k) \quad (2)$$

Further using various programming environments (Matlab, Mathcad, etc..) which make complex calculations sizes, can be determined for each  $k$  harmonic voltage, the current response size:

$$\underline{I}_k = c + jd = I_k (\cos \varphi_k + j \sin \varphi_k) \quad (3)$$

Considering unsaturated machine and applying the principle of superposition, the final value of the current results:

$$i = \sum_{k=1}^{\infty} \sqrt{2} I_k \sin(k\omega t + \alpha_k - \varphi_k) \quad (4)$$

The size of the load, therefore the machine load is given by sliding  $s$ .

### III. SIMULATION AND RESULTS

For example we took in consideration an low-power three-phase asynchronous motor with short circuit rotor with the following nominal parameters  $P_N = 1.1$  kW rated power,  $U_N = 380$  V rated voltage;  $I_{1N} = 2.75$  A-rated current,  $n_1 = 1500$  r.p.m., speed synchronism,  $M_N = 7425$  Nm nominal torque,  $s_N = 3.7\%$  nominal slip.

At nominal load  $P_2 = 1.1$  kW,  $P_1 = 1.288$  kW,  $Q_1 = 1.275$  kVAR,  $S = 1.813$  kVA,  $s_N = 3.7\%$ ,  $n_N = 1444$  r.p.m.,  $p_{Cu1} = 82.6$  W,  $p_{Cu2} = 43.2$  W,  $p_{Fepr} = 36.98$  W,  $p_{Fesup} = 0.56$  W,  $p_{m+v} = 24.7$  W,  $p_{Fes} = 0.55$  W,  $\Sigma p = 188.3$  W. In no load regime has resulted:  $P_2 = 0$ ,  $P_1 = \Sigma p_0 = 76.4$  W,  $p_{m+v} = 24.7$  W,  $s_0 = 0.5\%$ ,  $n_0 = 1492$  r.p.m.,  $M_0 = 0.165$  Nm. Sample heating by the method of two frequencies, means engine power from two different sources of voltages and frequencies (fig. 1).

#### A. Case I

The main source is the generator  $GS_I$  which is generating the voltage and base frequency  $U_I = 220$  V and  $f_I = 50$  Hz (figure 2.a). A study will be presented bellow to get the same losses as the nominal regime, resulting the auxiliary source  $GS_{II}$   $U_{II} = 73$  V,  $f_{II} = 45$  Hz (figure 2.a).

By connecting in series two sources will result in a voltage oscillator actual value  $U = 231.8$  V (fig. 2.b), so one size harmonic with period  $T = 0.2$  s and frequency  $f = 5$  Hz, (figure 2.c). Using numerical methods obtain the second harmonic  $U_9 = 73$  V,  $f_9 = 9.5 = 45$  Hz and  $U_{10} = 220$  V,  $f_{10} = 10.5 = 50$  Hz (fig. 2.d).

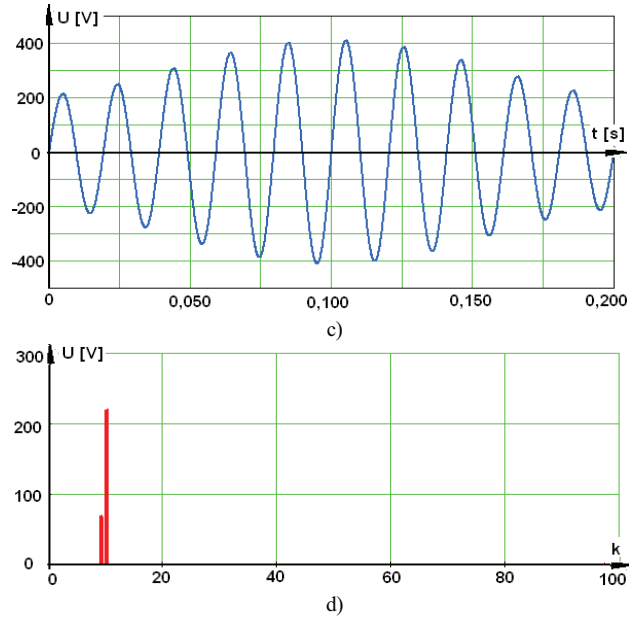
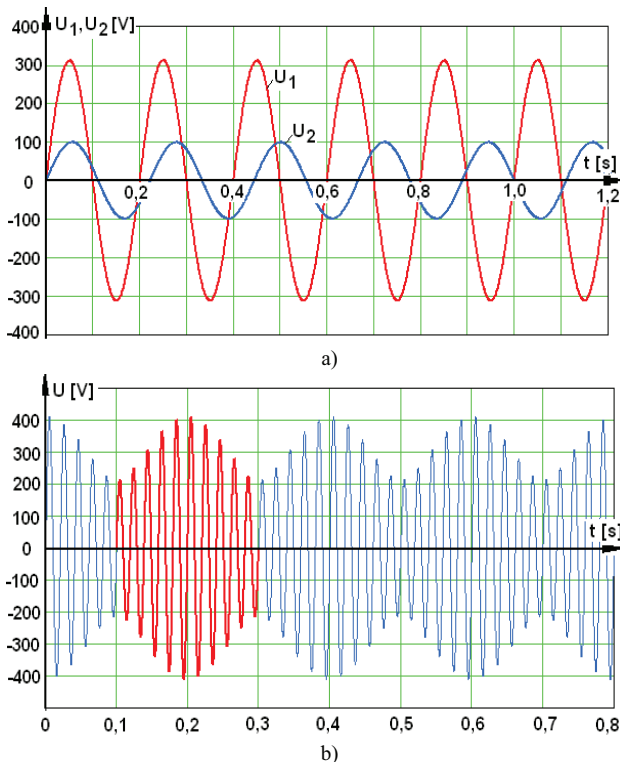


Fig. 2. Voltage curves: a) at the terminal of the two sources ; b) at the terminals of the motor ; c) the harmonic spectrum ;d) harmonic spectrum.

The mechanical characteristics corresponding to the two voltage values and different frequencies are shown in fig. 3.a noted with  $M_1$  and  $M_2$ . Considering rotor speed as variable, results  $s_I$  and  $s_{II}$  in the two speed fields  $n_I$  and  $n_{II}$  existing simultaneously in the machine.  $M_3$  in the notations of the mechanical characteristics correspondent to the rotor speed  $n$  and voltage  $U_{II}$  and  $M = M_1 + M_3$  is the final characteristic. Adequate to losses torque  $M_0 = 0.165$  Nm, from the motor characteristics represents  $din$  figure 3.b (shifted to the right) it result slid  $s_{00} = 3.0\%$  and speed  $n_{00} = 1455$  r.p.m. Motor speed at no load regime is imposed by the main source and at the same time the large inertia of the rotor creates small oscillation.

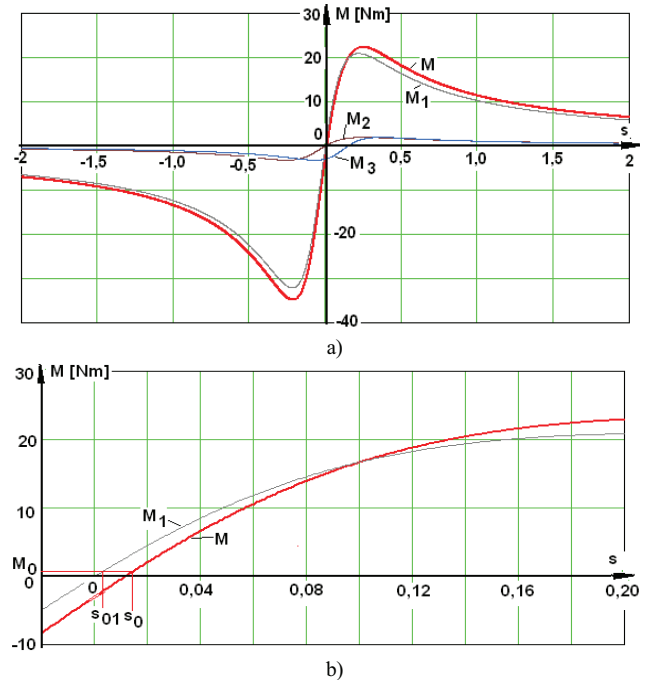


Fig. 3. Curves of the electromagnetic torques that appear in the machine: a)  $M_1$ ,  $M_2$  -created by the voltage  $U_I$ ,  $U_{II}$ ,  $M_3$  - torque compared to motors speed ,  $M$ - resulting torque; b) detail about identifying sliding on mechanical result characteristics.

Correspondent to no load function regime  $n_{00} = 1455$  r.p.m. is calculated the slid appropriate to the two fields  $s_{0I}$  and  $s_{0II}$ . Knowing the machine parameters  $R_1, R'_2, X_1, X'_2, X_{1m}$  (calculated for a frequency  $f_1 = 50$  Hz) and the sliding  $s_{0I}$  and  $s_{0II}$  obtained using the relations from the technical literature is determined the appropriate impedance for harmonic 9 and 10.

The results of the calculate current and phase voltage from the first source (fig. 4.a) are  $I_1 = 2.237$  A,  $\varphi_1 = 43.5^\circ$ , respectively to the second source (fig. 4.b),  $I_2 = 1.617$  A,  $\varphi_2 = 137.1^\circ$ .

The current from the motor (fig. 4.c, fig. 5.a) is obtained by graphical adding the two currents. The effective value of the current is  $I_{cr} = 2.757$  A the same as the nominal current of the motor. The current curve is represented in fig. 5.b and the harmonic spectrum in fig.5.c.

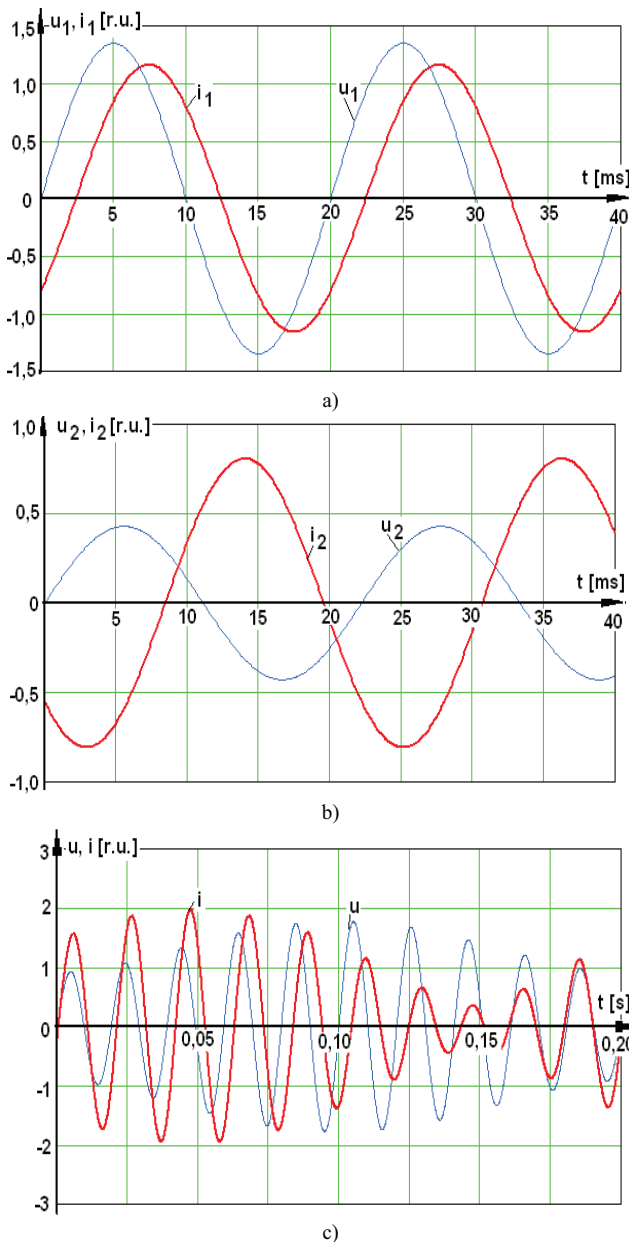


Fig. 4. Voltage and current curves at no load regime: a) at the terminal of  $GS_I$  source ; b) at the terminal of  $GS_{II}$  source; c) at terminal motor for one period.

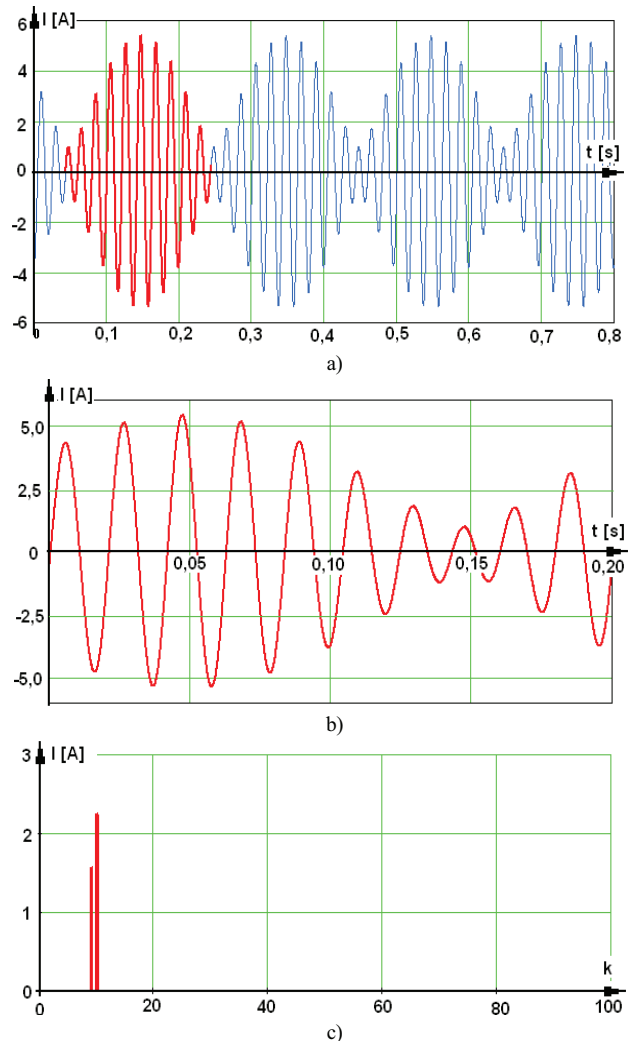


Fig. 5. Current curve at no load regime: a) at motor terminals; b) for a period; c) harmonic spectrum.

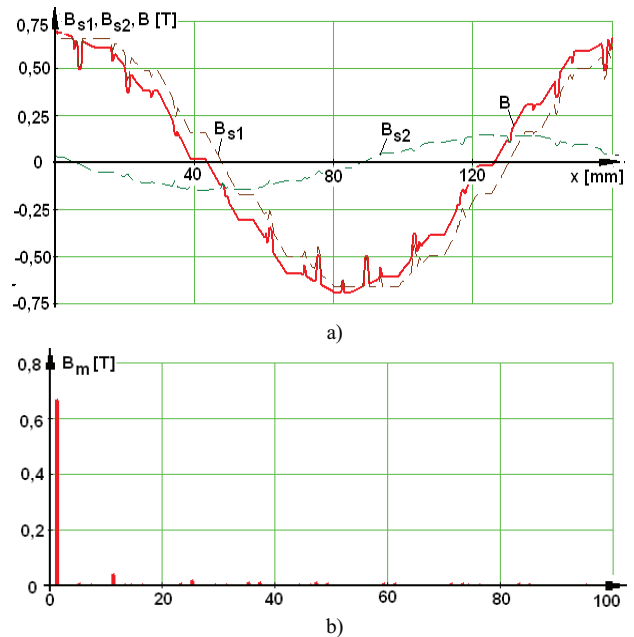


Fig 6. The air-gap flux density curves: a) due to the two sources and the resultant curve; b) harmonic spectrum waveform.

Using numerical and graphic methods for represents the magnetic fields [1], [6], [8-14], in fig. 6.a it was represented the distribution curves of the air-gap flux density on a pair of poles, when the machine is powered from the mains  $B_{s1}$ , from secondary source  $B_{s2}$  and the resultant curve B.

Harmonic analysis of magnetic field (fig. 6.b) shows that we have a fundamental harmonic and higher harmonics negligible importance. Note that the shape of the distribution curve is preserved, but the amplitude of the magnetic flux density changes periodically with the frequency  $f = 5$  Hz, as evidenced in fig. 7.a and 7.b. These large oscillations of the magnetic ( $B_{max} = 0.802$  T and  $B_{min} = 0.52$  T), means large oscillations of the electromagnetic torque and the speed diminished.

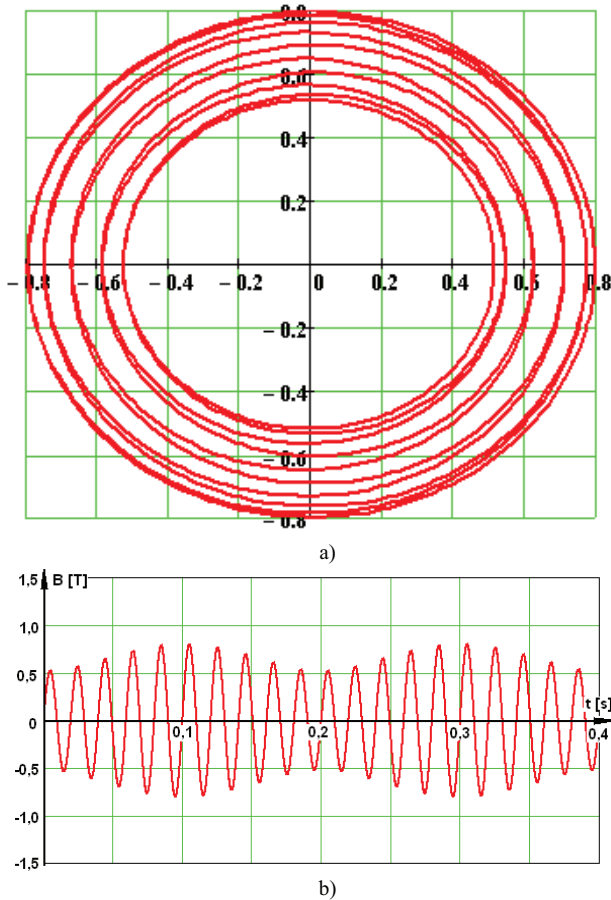


Fig.7. Phasor locus curve of magnetic induction  $B=f(\omega t)$ : a) for  $\omega t=(0 \div 10 \cdot 360^\circ)$ ; b) detail.

In Table no. I is listed, for comparison, the losses calculated for nominal load and the corresponding values obtained by the two frequencies method. From the results we see how the method of two frequencies the common iron core losses increase by 1.02% and total losses increase by 4.34%. As a result, the proposed method will obtained slightly higher temperatures in iron and stator winding.

Table no. I

Test method	Losses	$n_0$ (r.p.m.)	$P_{Cu}$ {W}	$P_{Fepr}$ {W}	$P_{Fes}$ {W}	$P_{m+iv}$ {W}	$\Sigma p$ {W}
Nominal Load		1444	123,6	36,9	0,56	17,8	178,86
The method of the two frequencies		1455	123,7	38,5	0,56	18,1	181,86

B. Case II

The main source remains the  $GS_I$  generator that provides voltage and core frequency,  $U_I = 220$  V,  $f_I = 50$  Hz, and the auxiliary source  $GS_{II}$  will have  $U_{II} = 185$  V,  $f_{II} = 47.5$  Hz. Is resulting an oscillating voltage effective value  $U = 290.8$  V (fig. 8), so one size harmonic with period  $T = 0.4$  s and frequency  $f = 2.5$  Hz.

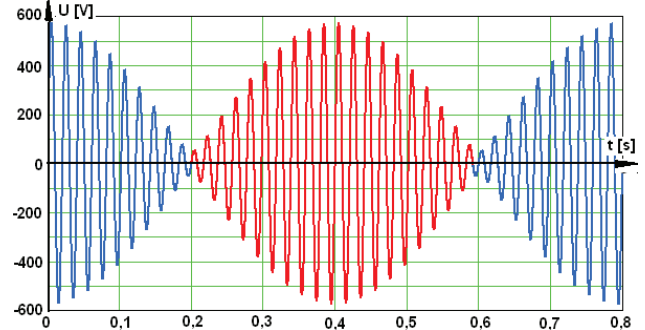


Fig 8. The curve of voltage at the terminals of the machine.

Following the above milestones, we resulting mechanical characteristics corresponding to the two different voltage and frequency values (fig. 9) noted with  $M_1$  and  $M_2$ . With  $M_3$  was noted the mechanical characteristic and rotor speed and voltage  $U_{II}$ , and with  $M=M_1+M_3$  resultant feature. Suitable torque  $M_0 = 0.165$  Nm, loss of characteristic result we slip  $s_{00} = 2.4\%$ , so the speed  $n_{00} = 1465$  r.p.m

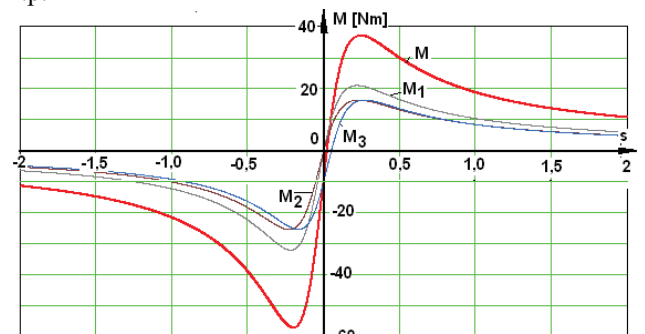


Fig.9. Electromagnetic torques curves appearing in the machine:  $M_1$ ,  $M_2$ , the data voltage and  $U_I$ ,  $U_{II}$ ,  $M_3$  -torque rotor speed relative to M-torque results.

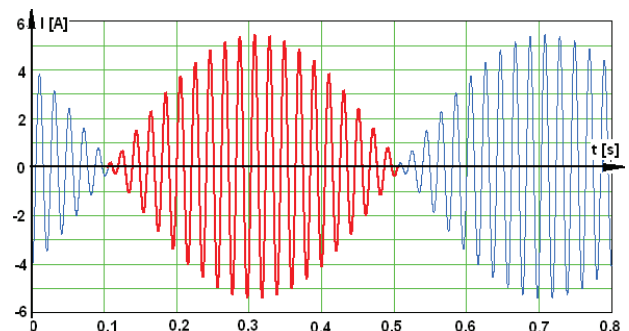


Fig 10. Current curve for the machine functioning with no load.

Correspondent for no load speed regime  $n_{00} = 1465$  r.p.m. we recalculate corresponding slides  $s_{0I}$  and  $s_{0II}$ , in both fields and determine the corresponding harmonic impedances 18 and 20.

We calculate the current and phase shift against voltage for first source  $I_1=1.97\text{ A}$ ,  $\varphi_1=47.5^\circ$ , respectively for second source  $I_2=1.87\text{ A}$ ,  $\varphi_2=129.1^\circ$ .

Current in the motor (fig. 10) is obtained by adding graphics currents from the two sources. The resultant current in the motor (fig. 10) is obtained by adding graphics currents from the two sources. The effective value of the current is  $I_{ef}=2.753\text{ A}$ , same with the rated motor current.

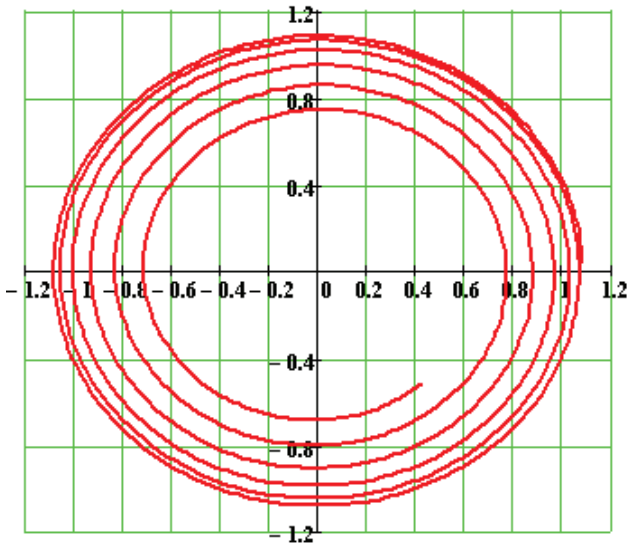


Fig. 11. Phasor locus curve of magnetic induction  $B=f(\omega t)$  for  $\omega t=(0\div 10\cdot 360^\circ)$ .

Looking at figure 11 we see that in this case we have much larger oscillations of the magnetic field ( $B_{max}=1.092\text{ T}$  and  $B_{min}=0.721\text{ T}$ ), the iron core losses increase by 14% and total to 4.8%. As a result, speed oscillations are increased, clearly the situation is more unfavorable than for case I.

C. Case III

The source still remains  $GS_I$  generator that provides voltage and core frequency,  $U_I=220\text{ V}$ ,  $f_I=50\text{ Hz}$ , and the auxiliary  $GS_{II}$  will have  $U_{II}=58\text{ V}$ ,  $f_{II}=42.5\text{ Hz}$ . Its resulting an oscillating voltage effective value  $U=233.2\text{ V}$  (fig. 12), so one size harmonic with period  $T=0.12\text{ s}$  and frequency  $f=8.33\text{ Hz}$ .

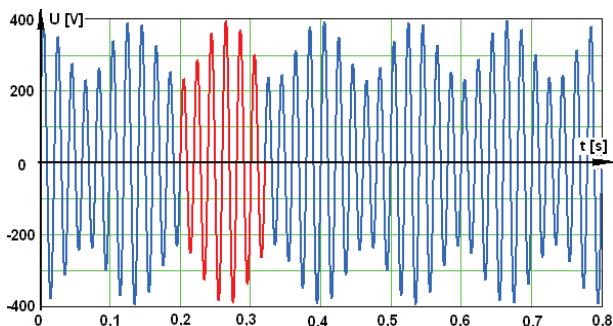


Fig. 12. The curve of voltage at the terminals of the machine.

We follow the steps in the I case, and are resulting mechanical characteristics corresponding to the two different voltage and frequency values (fig. 13) noted by  $M_1$  and  $M_2$ . We note with  $M_3$ , proper mechanical characteristic of rotor speed  $n$  and voltage  $U_{II}$ , and with  $M=M_1+M_3$  result-

tant feature. Corresponding to torque losses  $M_0=0.165\text{ Nm}$ , from machine characteristic we obtain the slip  $s_{00}=1.3\%$ , so the speed is  $n_{00}=1481\text{ r.p.m.}$

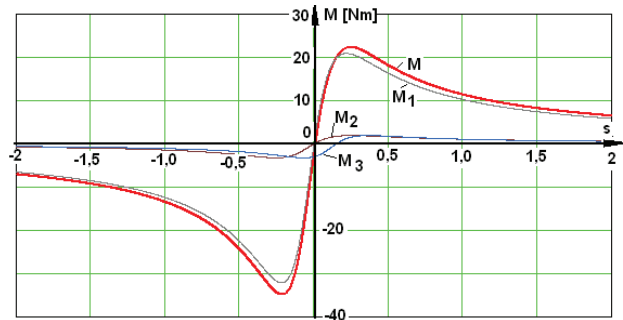


Fig. 13. Electromagnetic torques curves appearing in machine:  $M_1$ ,  $M_2$  – resulting on voltages  $U_I$ ,  $U_{II}$ , and  $M_3$  – the torque relative to rotor speed,  $M$  – resultant torque.

Corresponding to idling speed with no load  $n_{00}=1481\text{ r.p.m.}$  we calculate  $s_{0I}$  and  $s_{0II}$ , corresponding slides in the two fields, and determine the appropriate impedances harmonics 5 and 6.

We calculate current and phase shift against the voltage from the first source  $I_1=1.57\text{ A}$ ,  $\varphi_1=60.1^\circ$ , respectively second source  $I_2=2.25\text{ A}$ ,  $\varphi_2=125.6^\circ$ . Current in the motor (fig. 14) is obtained by adding graphics currents from the two sources. Effective current value is  $I_{ef}=2.746\text{ A}$ , very close to the rated motor current.

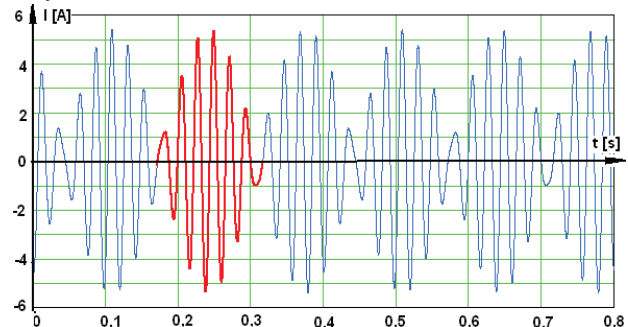


Fig. 14. Current curve for no load regime of the machine.

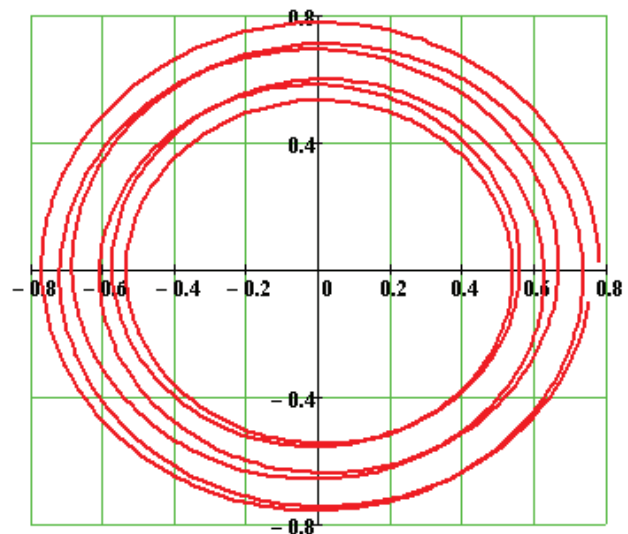


Fig. 15. Phasor locus curve of magnetic induction  $B=f(\omega t)$  for  $\omega t=(0\div 10\cdot 360^\circ)$ .

We can note that in this case we have much smaller oscillations of the magnetic field ( $B_{\max} = 0.796\text{T}$  and  $B_{\min} = 0.528\text{T}$ ), as a result the iron core losses increase by 3.6% and 1.1% total.

#### IV. CONCLUSIONS

A big difference between supply voltage frequencies, means losses corresponding to nominal regime, causing oscillations, so instability in the functioning of the group of machines.

If the frequencies are close, there are large oscillations of current and magnetic field resulting from machine

thus increasing iron losses that may influence heating of the machine.

The first method presented can establish the correct voltage and frequency of the auxiliary source for resultant losses in the machine, close to the nominal regime. In this way the synthetic sample heating can become conclusive.

#### REFERENCES

- [1] C.V. Aravind, I. Grace, T. Rozita, R. Rajparthiban, R. Rajprasad, Y.V. Wong, "Universal Computer aided Design for Electrical Machines", *Signal Processing and its Applications (CSPA) 2012*, pp.99-104.
- [2] C.U. Brunner, "International Standards for Electric Motors", *Standards for Energy Efficiency of Electric Motor Systems (SEEEM)*, 2007, pp. 6-10.
- [3] A. Câmpeanu, *Mașini electrice. Probleme fundamentale, speciale și de funcționare optimală*, Craiova, Ed. Scrisul Românesc, 1988.
- [4] A. Campeanu, I. Vlad, S. Enache, L. Augustinov, G. Liuba, I. Cautil, "Optimization of startup characteristics of medium power asynchronous motors with short circuit rotor", *ICEM'2012*, Marseille, France.
- [5] M. Centner, U. Schäfer, "Machine design software for induction machines," in *Proc. ICEM, Vilamoura*, Portugal, 2008, pp. 1-4.
- [6] I. Daniel, I. Munteanu, s.a., *Metode numerice in ingineria electrica*, Bucuresti, Editura MATRIX ROM, 2004.
- [7] O. Draganescu, *Incercarile masinilor electrice*, Bucuresti, Editura Tehnică, 1987.
- [8] J. Faiz, M.B.B. Sharifian, "Optimal design of three-phase Induction Motors and their comparison with a typical industrial motor", *Computers and Electrical Engineering*, vol. 27, 2001, pp. 133-144.
- [9] G. Liuba, M. Biriescu, "Incarcarea la incalzire a masinilor asincrone de mare putere prin metoda celor doua frecvente", *Conferinta Nationala de Electrotehnica si Electroenergetica*, Craiova, 1984.
- [10] D. Samarkanov, F. Gillon, P. Brochet, D. Laloy, "Techno-economic Optimization of Induction Machines: an Industrial Application", *ACEMP - Electromotion 2011*, Istanbul -Turkey, pp. 825-830.
- [11] V.M. Stanciu, M. Cistelean, V. Nitigus, M. Popescu, "Politics for the use of electric machines with high electric efficiency", *Electrical Engineering, Electronics and Automation Journal*, vol. 53, no. 3, 2005, Bucharest, Romania.
- [12] A. Taheri, A. Rahmati, S. Kaboli, "Energy Optimization of Field Oriented Six-Phase Induction Motor Drive", *AECE Journal*, Vol.11, Issue 2, Year 2011, pp.107-112.
- [13] T. Tudorache, L. Melcescu, "FEM Optimal Design of Energy Efficient Induction Machines", *AECE Journal*, Vol.9, Issue2, Year 2009, pp.58-64.
- [14] I. Vlad, A. Campeanu, S. Enache, Monica Enache, "Aspects regarding optimal design of high power squirrel cage asynchronous motors", *OPTIM 2012*, pp. 503 - 508.
- [15] I. Vlad, A. Campeanu, S. Enache, Monica Enache, "Aspects regarding design of squirrel cage asynchronous motors for mining excavators", *Annals of the University of Craiova, Series Electrical Engineering*, Year 36, No. 36, 2012, pp. 57-62.
- [16] \*\*\* CEI 60034-2-1 Standard, "Rotating electrical machines-Part 2-1", *Standard methods for determining losses and efficiency from tests*, Edition 1.0, 2007.